U.S. DEPARTMENT OF ENERGY | Office of Science

DOE/SC-ARM-15-053

Atmospheric Line of Site Experiment (ALOSE) Final Campaign Summary

W Smith
S Green
M Howard
M Yesalusky
N Modlin

March 2016

ARM
CLIMATE RESEARCH FACILITY

DISCLAIMER

This report was prepared as an account of work sponsored by the U.S. Government. Neither the United States nor any agency thereof, nor any of their employees, makes any warranty, express or implied, or assumes any legal liability or responsibility for the accuracy, completeness, or usefulness of any information, apparatus, product, or process disclosed, or represents that its use would not infringe privately owned rights. Reference herein to any specific commercial product, process, or service by trade name, trademark, manufacturer, or otherwise, does not necessarily constitute or imply its endorsement, recommendation, or favoring by the U.S. Government or any agency thereof. The views and opinions of authors expressed herein do not necessarily state or reflect those of the U.S. Government or any agency thereof.

DOE/SC-ARM-15-053

Atmospheric Line of Site Experiment (ALOSE) Final Campaign Summary

W Smith, Sr., Hampton University/University of Wisconsin-Madison
Principal Investigator

S Green, Aerospace Consultant
M Howard, National Security Technologies LLC
M Yesalusky, Hampton University/National Security Technologies LLC
N Modlin, Aerospace Corporation
Team Members

March 2016

Work supported by the U.S. Department of Energy,
Office of Science, Office of Biological and Environmental Research

Summary

The Atmospheric Line of Site Experiment (ALOSE) was a project to produce best-estimate atmospheric state measurements at the:

1. DOE Atmospheric Radiation Measurement (ARM) Clouds and Radiation Test-bed (CART) site located in Lamont, Oklahoma (11–14 December 2012)
2. Poker Flat Alaska Research Range (PFRR) located in Poker Flat, Alaska (19–26 February 2013)
3. DOE ARM CART site located in Lamont, Oklahoma (24–28 April 2013)
4. DOE ARM CART site located in Lamont, Oklahoma (9–15 July 2013)
5. DOE ARM Tropical Western Pacific (TWP) site located in Darwin, Australia (27 September–3 October 2013).

The ALOSE was conducted through deployments at three different research sites for five different climate regimes and seasons (months):

1. U.S. Southern Great Plains (SGP) ARM site—mid-latitude continental
    a. Autumn/winter (December 2012)
    b. Spring (April 2013)
    c. Summer (July 2013)
2. Poker Flat, Alaska, Geophysical Research site—high-latitude continental
    a. Winter (February 2013)
3. TWP ARM site—low-latitude oceanic
    a. Equinox (September 2013)

During these deployments, measurements were obtained from: (1) a surface meteorological station, (2) radiosondes (i.e., balloon soundings), (3) four different satellites (i.e., Aqua, Suomi-NPP, and Metop-A, and Metop-B) carrying hyperspectral vertical sounding sensors (AIRS, CrIS, and IASI), and (4) the AERI and the ASSIST hyperspectral radiance spectrometers viewing upward at the atmosphere. The on-site AERI measured the radiation continuously in the zenith (i.e., vertical) viewing direction, while the ASSIST conducted measurements at the four different local zenith angles (0, 30, 45, and 60 degrees) and each of four azimuth angles (0, 90, 180, and 270). The ASSIST measurements were obtained quasi-continuously, dependent on weather, and thus were generally coincident with the satellite overpass times. Radiosonde measurements were conducted at the normal 2330 and 1130 UTC, as well as at intermediate times providing a frequency as high as 3-hour intervals. Satellite data from Aqua AIRS, Suomi-NPP CrIS, and Metop-A/-B IASI during overpasses of the experiment sites were collected during each deployment, used in the production of atmospheric profiles from the ASSIST spectral radiance data, and made part of the ALOSE archived data sets. The atmospheric profile retrievals from the satellite hyperspectral sounder (i.e., AIRS, CrIS, and IASI) radiance data provided temperature and moisture profile information, along with the radiosonde balloon soundings, within the free troposphere and stratosphere, which is beyond the sensing capability of the AERI and the ASSIST instruments.

This is the final report describing the ALOSE project. It provides (1) the preparation and deployment logistics for each of the five experiments; (2) the results of radiance calibration validation performed during each experiment; (3) the methodology used for combining the surface data, satellite profiles, radiosonde profiles, and the ASSIST radiance spectra for providing an optimal depiction of the atmospheric state along the four zenith angle and four azimuth angle viewing directions; (4) provides example displays of vertical cross sections and comparisons of the ASSIST-derived atmospheric profile retrievals with simultaneous radiosonde measurements for each ALOSE deployment, including comparisons of the NOAA Global Forecast System (GFS) analysis/forecast product with the ALOSE product; and (5) provides a description of the archive of the data collected and provided on a DVD, available upon request from the DOE ARM project.

Acronyms and Abbreviations

AERI	Atmospheric Emitted Radiance Interferometer
AFWA	Air Force Weather Agency
ALOSE	Along Line Of Site Experiment
ARM	Atmospheric Radiation Measurement
ASSIST	Atmospheric Sounder Spectrometer for Infrared Spectral Technology
CART	clouds and radiation test-bed
DOE	U.S. Department of Energy
GFS	Global Forecast System
LBLRTM	Line-By-Line Radiative Transfer Model
PBL	planetary boundary layer
PFRR	Poker Flat Research Range
RAQMS	Real-time Air Quality Modeling System
SGP	Southern Great Plains
TWP	Tropical Western Pacific

Contents

Figures

1.0 Background

The Atmospheric Line of Site Experiment (ALOSE) was a project to produce best-estimate atmospheric state measurements, which could be used to validate forecast model produced line-of-site atmospheric structure estimates. These estimates and associated model validations represent atmospheric conditions ranging from warm moist tropical air masses to dry winter polar air masses. In order to obtain this large range of atmospheric conditions, measurement campaigns were held at the:

1. DOE Atmospheric Radiation Measurement (ARM) Clouds and Radiation Test-bed (CART) site located in Lamont, Oklahoma (11–14 December 2012)
2. Poker Flat Alaska Research Range (PFRR) located in Poker Flat, Alaska (19–26 February 2013)
3. DOE ARM CART site located in Lamont, Oklahoma (24–28 April 2013)
4. DOE ARM CART site located in Lamont, Oklahoma (9–15 July 2013)
5. DOE ARM Tropical Western Pacific (TWP) site located in Darwin, Australia (27 September–3 October 2013).

The main participants in the ALOSE measurement campaigns were William Smith Sr. (Principal Investigator, Hampton University and University of Wisconsin-Madison), Stan Green (Aerospace Consultant), Michael Howard (NSTec), Melissa Yesalusky (Hampton University, NSTec), and Norman Modlin (Aerospace Corperation).

During these deployments, measurements were obtained from: (1) a surface meteorological station, (2) radiosondes (i.e., balloon soundings), (3) four different satellites (i.e., Aqua, Suomi-NPP, and Metop-A, and Metop-B) carrying hyperspectral vertical sounding sensors (AIRS, CrIS, and IASI), and (4) the AERI and the ASSIST (Rochette et al. 2009) hyperspectral radiance spectrometers viewing upward at the atmosphere. The on-site AERI measured the radiation continuously in the zenith (i.e., vertical) viewing direction while the ASSIST conducted measurements at the four different local zenith angles (0, 30, 45, and 60 degrees) and each of four azimuth angles (0, 90, 180, and 270). The ASSIST measurements were obtained quasi- continuously, dependent on weather, and thus were generally coincident with the satellite overpass times. Radiosonde measurements were conducted at the normal 2330 and 1130 UTC, as well as at intermediate times, providing a frequency as high as 3-hour intervals. The ASSIST measurements are important for observing the diurnal variation of the thermodynamic structure of the Planetary Boundary Layer (Smith et al. 1999).

The retrieval of atmospheric profiles from ASSIST radiance measurements is performed using a physically based optimal estimation (Rodgers 1976) (see: http://en.wikipedia.org/wiki/Optimal_estimation) procedure followed by a direct simultaneous numerical inversion of the radiative transfer equation using the optimal estimation profile as the initial condition and constraint for the matrix inversion process. Specifically, the optimal estimation solution is defined in Eq. (1) as

$$q_r = q_o + (r_m - r_o)C \tag{1}$$

where q = a vector containing the atmospheric profile quantities
r = a vector containing the radiance spectrum

C = the solution matrix, which comprises the statistical covariance of radiance spectra, profile quantities, and radiance observation error about the statistical sample mean or initial guess condition.

The subscripts *r*, *o*, and *m* refer to the retrieval, initial condition, or mean of the profiles comprising the statistical sample utilized, and the measurement, respectively. The solution matrix, C, is computed using Eq. (2)

$$C = \left(R'^T R' + \lambda E^T E \right)^{-1} R'^T Q' \tag{2}$$

where *Q* and *R* are climatological matrices whose elements consist of a climatological ensemble of atmospheric profile values and ASSIST spectral radiances calculated using a Line-By-Line Radiative Transfer Model (LBLRTM). The prime symbol indicates the deviation from the climatological mean profile or initial profile conditions, q_o and r_o. The error covariance matrix, $E^T E$, is diagonal assuming random spectral measurement noise with the Lagrangian multiplier, λ, used to stabilize the matrix inversion.

The statistical sample of atmospheric profiles used to generate the matrix C is generally determined from a global set of climatological profiles generated by the NOAA Real-time Air Quality Modeling System (RAQMS) (Pierce et al. 2003). However, for the ALOSE experiments, a subsample of atmospheric profiles for the local region and season, taken from the 2010 RAQMS database, were used to compute the **"C"** matrix of Eq. (2). Retrievals are obtained in the presence of cloud by using **"C"** matrices computed for 11 different profile retrievals, one for each of ten different assumed cloud base pressure altitude conditions (i.e., 970, 950, 910, 860, 780, 700, 620, 450, 250, and 125 hPa) and one for the clear condition. The retrieval coefficients were pre-computed using the LBLRTM for the ten cloud base altitudes assuming an opaque overcast condition for each sounding in the statistical data set, as well as a clear sky condition for each sounding. Because the retrieval for each cloud height class is linear, the statistics are able to represent any cloud amount/emissivity condition between the natural limits of zero and unity. The correct cloud base height and associated retrieval is selected from the 11 possible solutions as that retrieval which agrees best, in an RMSD sense, with an a priori background atmospheric state based on forecast model, satellite, and radiosonde data, as discussed below.

The retrieval methodology for deriving these vertical profile data for ALOSE is based on the technique outlined above but using a background, or initial profile, based on the analysis of all available satellite and radiosonde measurements obtained during the entire day of observation. The ALOSE algorithm flow diagram is shown in Figure 1. Basically, a statistical database, obtained from the output of the RAQMS for the year 2010, is used within a statistical regression retrieval algorithm to provide an initial estimate of the thermodynamic and trace gas profiles. For ALOSE, a final retrieval of these profiles is then achieved using a physical regression retrieval algorithm where the statistical bias in the initial pure regression estimated profiles is determined by the comparison of a second statistical retrieval based on radiances simulated from real-time RAQMS chemistry and Global Forecast System (GFS) model thermodynamic (i.e., temperature and water vapor) forecasts, modified using ALOSE satellite and radiosonde data, for the time and location of the ASSIST measurements. The bias correction is simply the difference between the regression retrieval obtained from the simulated radiances and the Model+Satellite+Radiosonde (RSR) analysis profile used to simulate the radiance spectrum used for the second retrieval. This statistical bias correction, RSR analysis profile minus RSR simulated ASSIST radiance retrieved profile, is then added

to the original observed ASSIST radiance retrieved profile. The elements of the retrieval procedure used for ALOSE are summarized as follows:

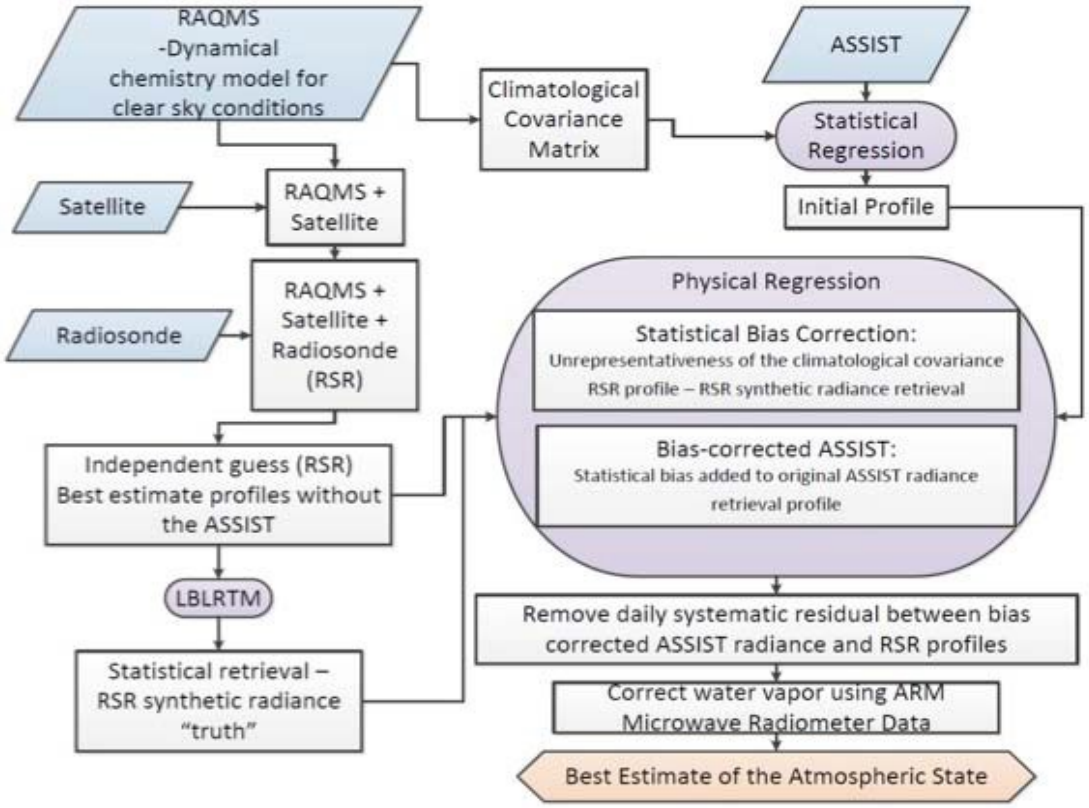

Figure 1. Flow diagram for the ALOSE sounding retrieval algorithm.

1. An initial profile is obtained from the ASSIST radiance observations by optimal estimation using climatological covariance matrices produced by the global RAQMS dynamical chemistry model for clear sky conditions.
2. An independent guess of the temperature and moisture structure is then obtained from the combination of real-time RAQMS and GFS combined model output modified through the incorporation of satellite profiles over the ALOSE measurement site and radiosondes released from the ALOSE measurement site (RSR). This independent guess (RSR) is believed to be the best estimate of the atmospheric structure without the use of the ASSIST radiance spectra.
3. A second optimal estimation profile retrieval is then obtained from an ASSIST radiance spectrum calculated using the LBLRTM with the RSR profile used as the input atmospheric profile. Because the "truth" for this second retrieval is known (i.e., the RSR profile used to produce the second retrieval), the error in the retrieval resulting from the unrepresentativeness of the climatological covariance used (called the "statistical bias") is then estimated as the difference between the RSR profiles and the RSR synthetic radiance retrievals.
4. A "statistical bias"-corrected ASSIST retrieval is then obtained by adding the "statistical bias" profile to the initial observed ASSIST spectral radiance optimal estimation retrieval.

5. The final profile retrieval result is obtained by removing any daily mean systematic residual between the bias-corrected ASSIST radiance retrieval obtained in step 4 and the RSR atmospheric profiles for the radiosonde measurement times.

The procedure outlined above is expected to produce the best estimate of the atmospheric state for the ASSIST measurement times and local zenith and azimuth angles of measurement based on all sources of atmospheric data obtained at the ALOSE measurement site as required for validating forecast model produced line-of-site atmospheric structure estimates.

Figures 2, 3, and 4 show as an example the comparison between the temperature cross sections constructed from the Model data, the Model data with the satellite profile data added, the Model data with both satellite and radiosonde data added, and the final ASSIST retrieval product. The final ASSIST enhanced Model+Satellite+Radiosonde products are shown in the next section. As can be seen, more detail in the representation of the atmospheric structure is obtained through the addition of different

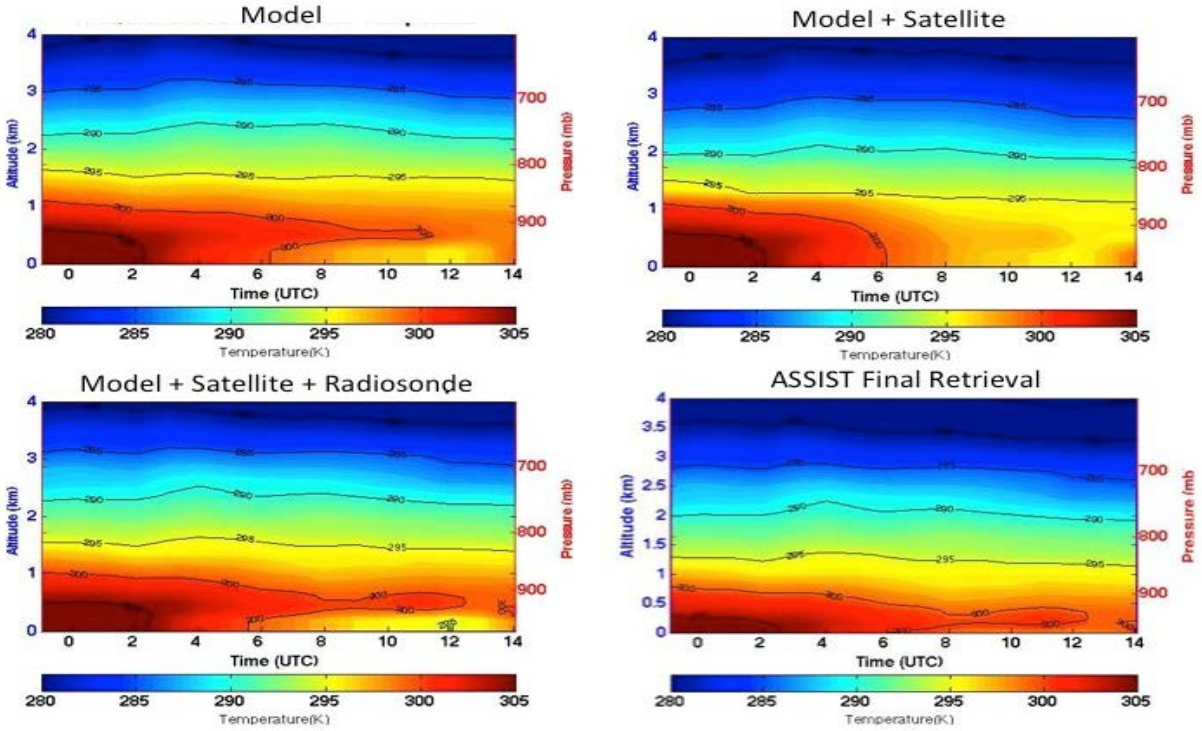

Figure 2. Comparison between cross sections of analyzed temperature. The upper left panel is for the Model analysis, the upper right panel is for the satellite data added to the Model analysis, the lower left panel is for the radiosonde data added to the satellite analysis, and the lower right panel is the analysis of the final ASSIST retrievals.

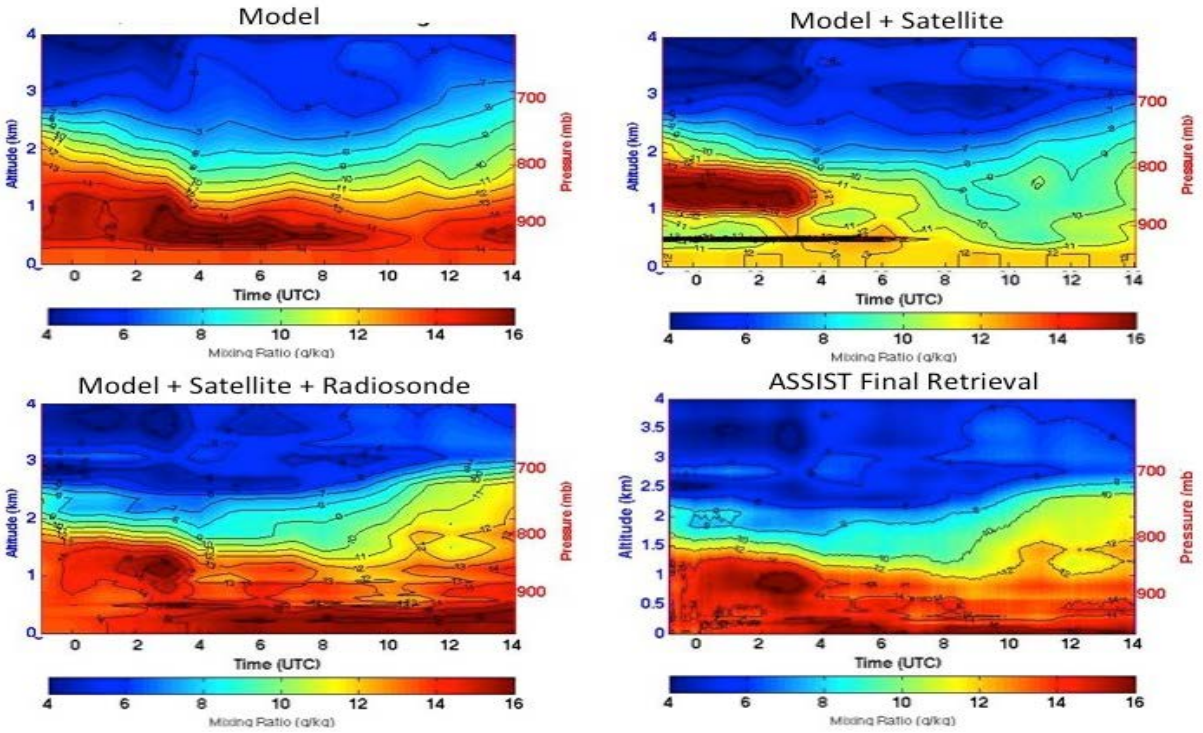

Figure 3. Same as Figure 2 but for mixing ratio.

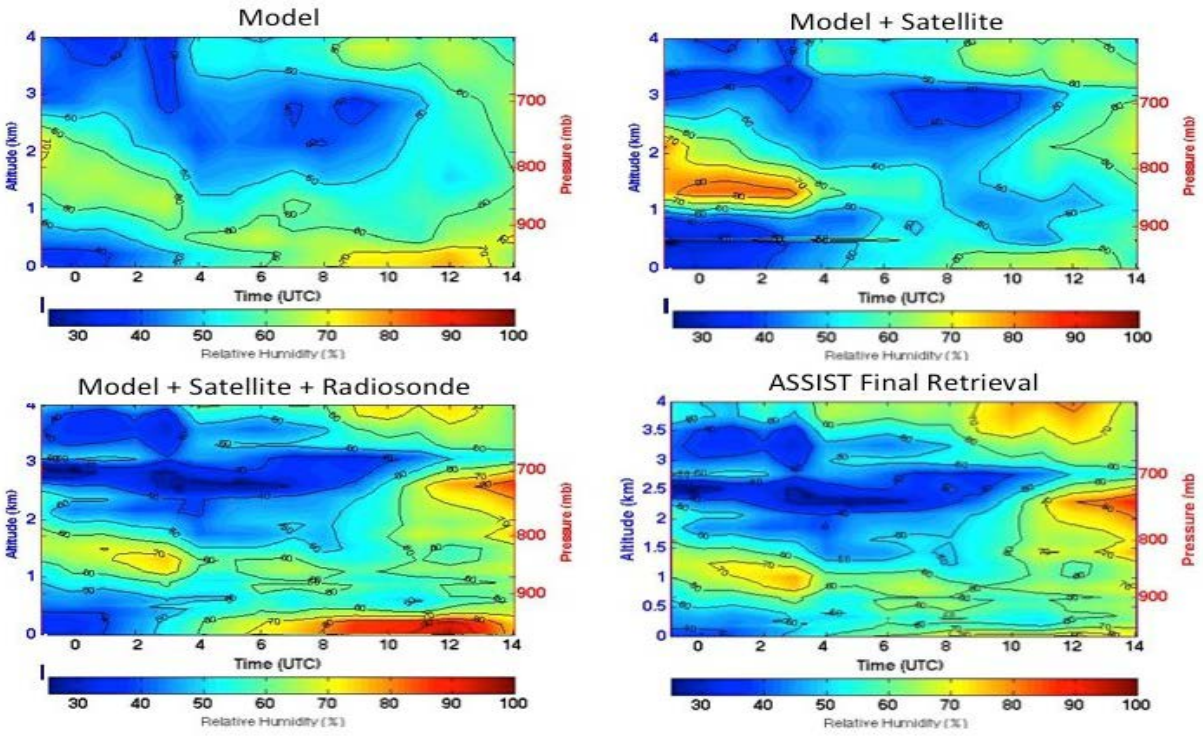

Figure 4. Same as Figure 2 but for relative humidity.

observations in each step of the retrieval process. The ASSIST Final Retrieval product is believed to be the most accurate result and is shown to agree with the radiosonde measurement to within the general accuracy of the radiosonde measurements.

2.0 Notable Events or Highlights

- **ALOSE 1:** Results showed significant diurnal variability of the PBL but little zenith and azimuthal dependence on profile observations. This is believed to be the result that the ASSIST can only see a volume of air having a 1–2 km radius about the instrument location.
- **ALOSE 2:** Numerical forecast results for the Alaskan region have significantly larger errors than at lower latitude, particularly for moisture. The ALOSE measurement analysis scheme was able to resolve the diurnal variation of the very large low-level inversion, which varied in amplitude from near zero to 20 degrees Celsius.
- **ALOSE 3:** The ASSIST data was able to resolve a high degree of vertical moisture structure within the PBL at the ARM SGP site during April. Also, the diurnal and day-to-day variation of atmospheric moisture was relatively large during this spring period of observation.
- **ALOSE 4:** The summertime ASSIST measurements at the ATM SGP site revealed significant variations in low-level moisture and atmospheric stability associated with the onset of convection and associated thunderstorms. During these pre-convective periods, a significant dependence of the profile results on the viewing direction of the ASSIST instrument could be seen.
- **ALOSE 5:** At Darwin, little variation in atmospheric temperature was observed during the experiment period and the GFS model panels compared favorably with the final ASSIST panels. However, the model humidity deviates significantly from the final ASSIST product. It was generally seen that the final ASSIST product revealed a lot of moisture structure not shown by the model but validated by the high-frequency radiosonde profile data obtained at the Darwin TWP ARM site.
- There were two major instrument issues, which surfaced during the ALOSE campaigns. The first dealt with the sun getting into the telescope within an hour of noon at the SGP site in July, while the second was the failure of the ASSIST internal air conditioning system at Darwin. The first issue was resolved by simply making sure that the ASSIST scan mirror was not pointed in the direction of the sun when the sun was high in the sky. The second issue was resolved by using a room air condition to keep the instrument cool when operating during the hot afternoon hours of the day at Darwin.

3.0 Lessons Learned

Everything went well for all five deployments. The only problem was the breakage of the ASSIST enclosure internal air conditioning system during its shipment to Darwin, Australia. This system was replaced with a much more robust system for future deployments.

4.0 Results

ALOSE ground truth data was produced using forecast model, satellite, conventional surface and radiosonde, and quasi-time-continuous ASSIST radiance observations made for five different climate regimes:

- Continental U.S. Southern Great Plains (SGP) autumn/winter (December 2012)
- Poker Flat, Alaska Arctic winter (February 2013)
- Continental U.S. SGP spring (April 2013)
- Continental U.S. SGP summer (July 2013)
- TWP Australia equinox (September 2013)

The quality of the data gathered is excellent with the final ASSIST/satellite/radiosonde atmospheric product providing the fine-scale vertical and temporal structure of the atmosphere. Comparisons of the final product with the GFS analysis/forecast model product reveals the deficiencies of a relatively low spatial (111 km) and temporal (6 hr) resolution model product to capture important fine-scale vertical and temporal variation features of the tropical atmosphere, especially for moisture. There were several measurement days where the angular variation of the observations proved valuable in measuring the spatial variation of atmospheric conditions within the PBL. The ALOSE data set is expected to prove to be invaluable for its intended purpose of validating the accuracy of the atmospheric state predicted by the Air Force Weather Agency (AFWA) prediction models, as well as for validating satellite remote sensing data obtained over the globe for different weather and climate regimes.

Below is a summary of the results for each experiment provided together with a discussion of the information gained from the observations.

4.1 ALOSE-1

Figure 5 shows the temperature and humidity time section inputs (i.e., GFS model, satellite, and radiosonde) for obtaining the final ASSIST best estimate of the atmospheric state of the lower troposphere (0–4 km) for ALOSE-1; 11, 12, 13, and 14 December. The digital data for atmospheric temperature, mixing ratio, and relative humidity are obtained at 60 levels ranging between the surface and the 2 hPa pressure level, with a time spacing of 2.3 minutes. The white areas in these figures denote missing data due to cloud obstruction. As shown in Figure 5, the atmosphere became warmer and less humid during the period between 11 December and 13 December, with 14 December being slightly cooler and slightly more humid than 13 December. It can also be seen that the ASSIST data influences the final humidity product much more than any other data source. This result was expected because of the fine-scale variations in atmospheric humidity that are not resolved by the lower vertical resolution model and satellite data and the poor temporal resolution radiosonde data. In any case, the final ASSIST product represents the best estimate of the atmospheric temperature and water vapor state of the atmosphere available from all sources of data.

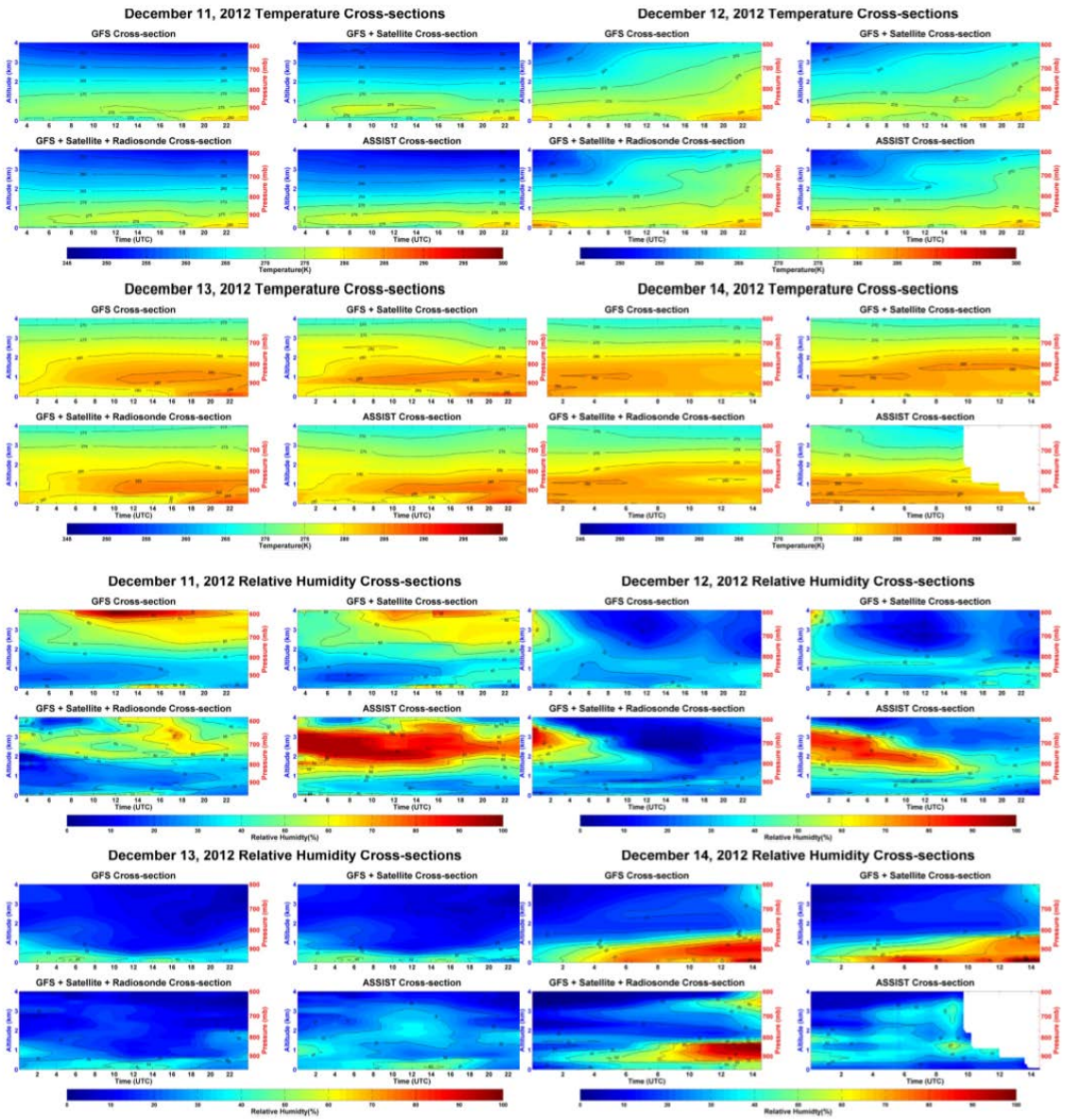

Figure 5. Temperature and humidity time section inputs (i.e., GFS model, satellite, and radiosonde) for obtaining the final ASSIST best estimate of the atmospheric state of the lower troposphere (0–4 km) for ALOSE-1; 11, 12, 13, and 14 December.

Figure 6 show time cross sections of the final ALOSE-1 ASSIST temperature and humidity profile deviations from the daily profile mean for the four different local zenith angles of measurement (0, 30, 45, and 60 degrees) with the indication of which of the four different azimuth angles (west, south, east, north) of the observation shown at the top of each figure.

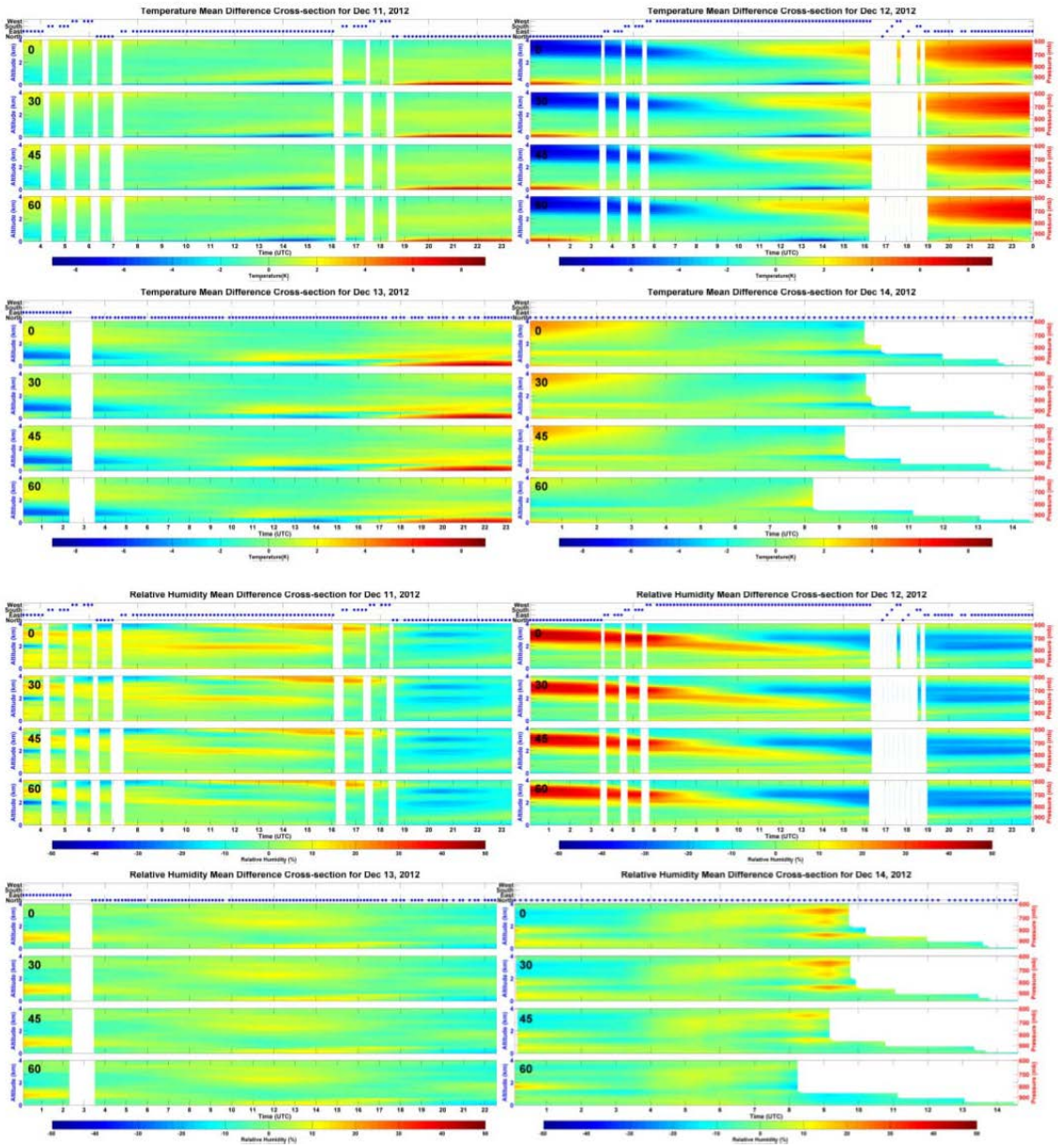

Figure 6. Time cross sections of the final ALOSE-1 ASSIST temperature and humidity profile deviations from the daily profile mean for the four different local zenith angles of measurement (0, 30, 45, and 60 degrees) with the indication of which of the four different azimuth angles (west, south, east, north) of the observation being viewed shown at the top of each figure.

The profile data is presented in this manner as an attempt to depict any significant dependence of the atmospheric state on the viewing direction. In principle, as the local zenith angle of measurement is increased, the feature at a certain time and altitude should be further away from the instrument than the same feature observed at a smaller local zenith angle, the feature being directly overhead for a local zenith angle of zero degrees. Changing the local azimuth angle of measurement also serves to depict any horizontal inhomogeneity of the atmosphere. As can be seen for the ALOSE-1 measurement days, the atmosphere was horizontally homogeneous in that there is little, if any, dependence on the local zenith and azimuth angles of measurement, at least within the limited 2–3 km radius spatial measurement

sensitivity volume surrounding the ASSIST instrument. On the other hand, the correspondence of these ASSIST products for all local zenith angles of measurement indicate a very high accuracy of these profile products.

Figure 7 shows an example of the correspondence of the final ASSIST profiles to the radiosonde observations. It can be seen that the ASSIST product closely resembles the radiosonde observation, particularly for temperature, but is not forced to agree with it as is evident from the discrepancies between the ASSIST and radiosonde humidity profiles where the ASSIST shows more large-scale vertical variability than does the radiosonde.

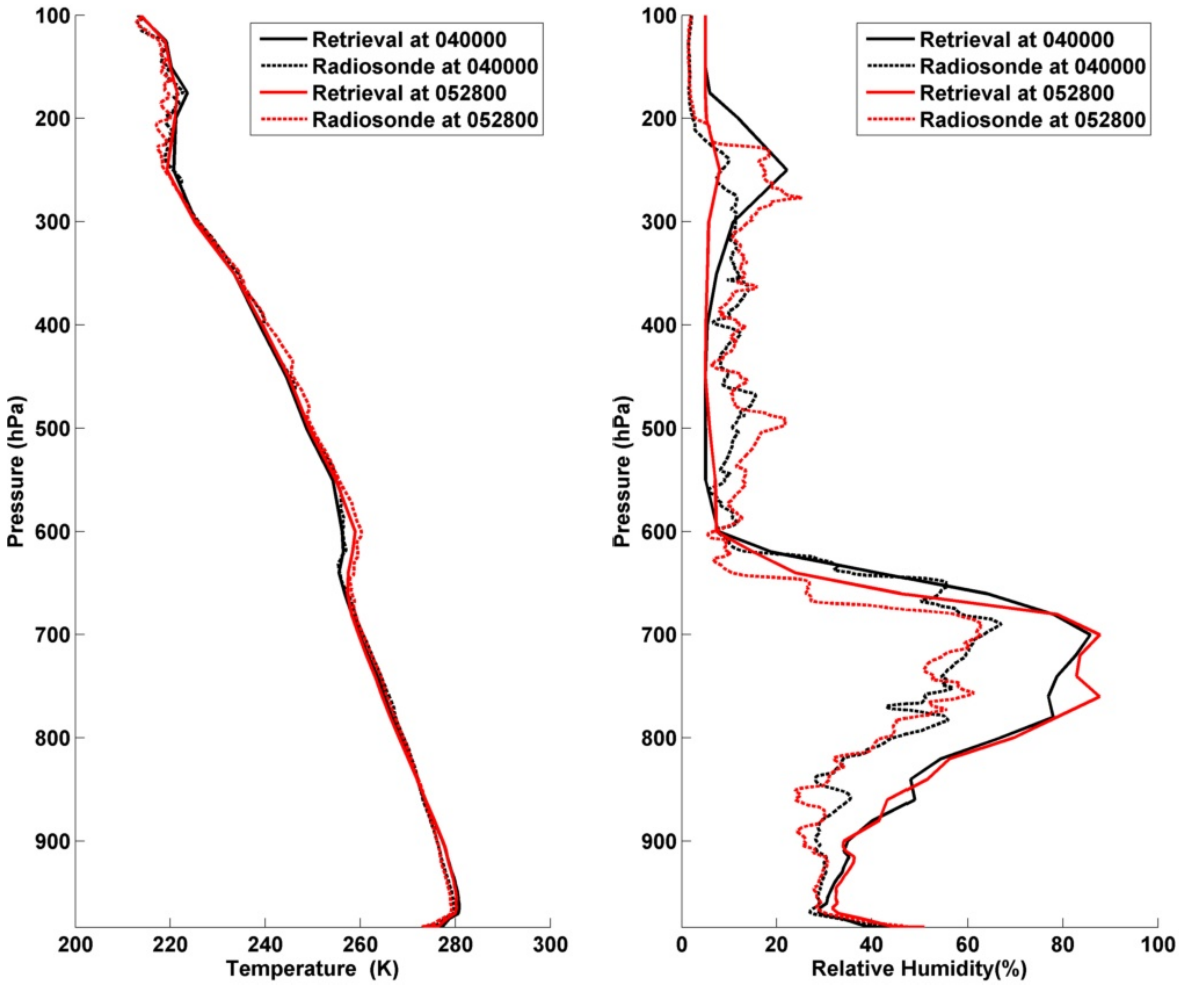

Figure 7. Comparison of the ASSIST profile product with radiosonde measurements 1.5 hours apart at the DOE SGP ARM CART site on 11 December 2012.

4.2 ALOSE-2

Figure 8 shows temperature and humidity time section inputs (i.e., GFS model, satellite, and radiosonde) for obtaining the final ASSIST best estimate of the atmospheric state of the lower troposphere (0–4 km) for ALOSE-2; 19, 20, 23, and 26 February.

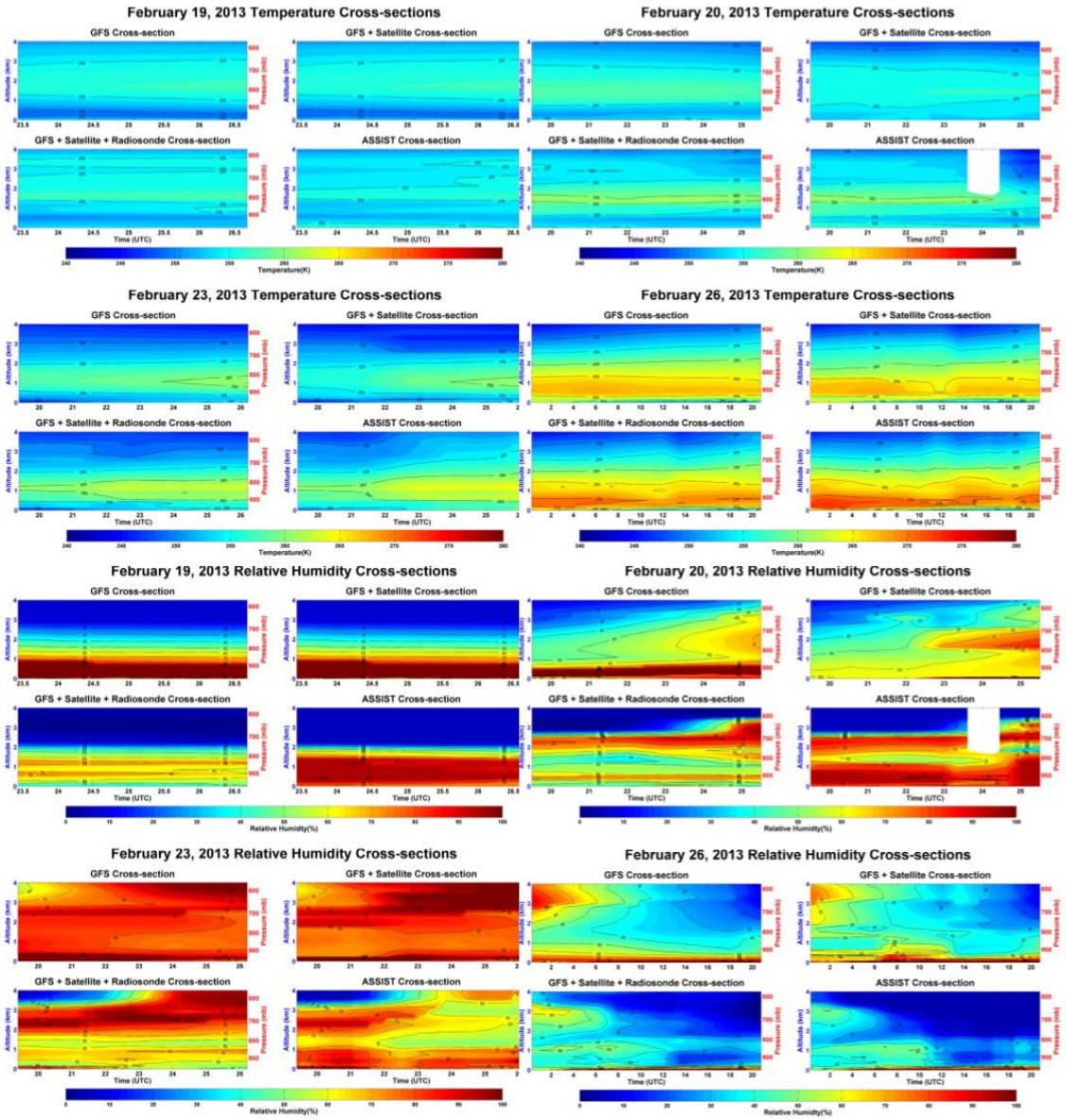

Figure 8. Temperature and humidity time section inputs (i.e., GFS model, satellite, and radiosonde) for obtaining the final ASSIST best estimate of the atmospheric state of the lower troposphere (0–4 km) for ALOSE-2; 19, 20, 23, and 26 February.

As can be seen, the temperature is coldest at the beginning of the measurement period and warmest at the end. Most interesting is the fact that the model and satellite data do not capture the strength of the low-level inversion shown distinctly in the radiosonde and ASSIST cross sections, most evident for 20 and 23 February. The ASSIST seems to provide unique information for the low-level water vapor, being significantly different than that shown by the model, satellite, and in some cases even the radiosonde, cross sections.

Figure 9 shows a comparison between the final ASSIST retrieved temperature profile and the radiosonde for 25 February when a strong low-level inversion existed. As can be seen the strength of the inversion shown by the radiosonde is captured quite well in the final ASSIST retrieval, although there are some significant differences (i.e., 2–3 degrees) in the absolute temperature values.

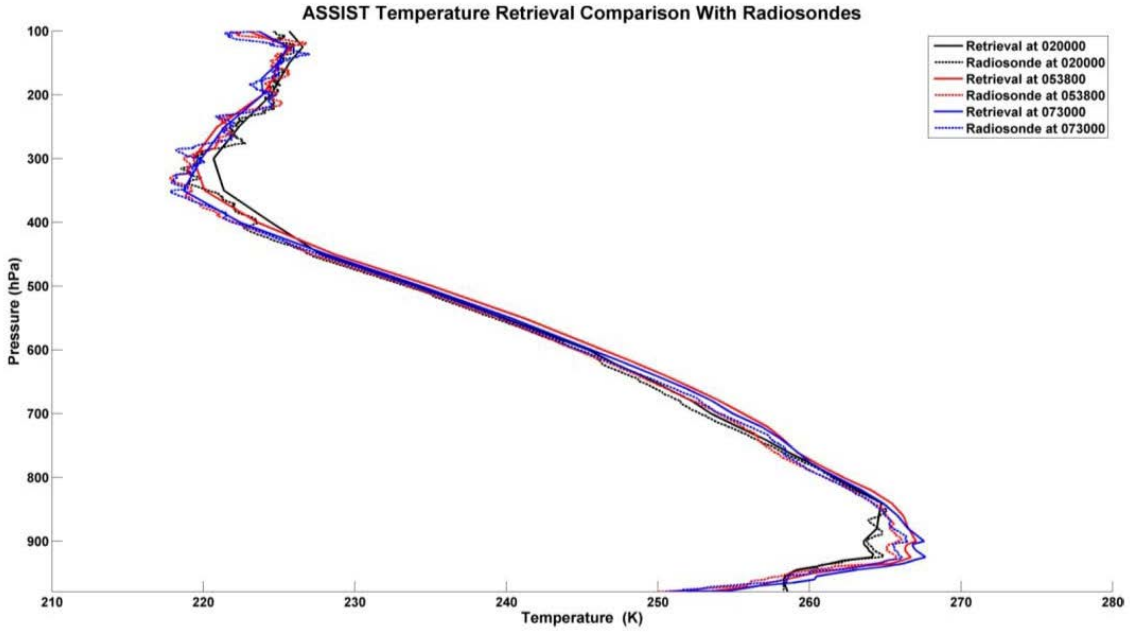

Figure 9. Comparison of final ASSIST temperature profile retrievals and radiosonde profile measurements at Poker Flat, Alaska, for three different radiosonde release times during 25 February 2013.

Figure 10 shows time cross sections of the final ALOSE-2 ASSIST temperature and humidity profile deviations from the daily profile mean for the four different local zenith angles of measurement (0, 30, 45, and 60 degrees) with the indication of which of the four different azimuth angles (west, south, east, north) of the observation shown at the top of each figure. Unlike ALOSE-1, for the Arctic data of ALOSE-2 we do see some significant dependence on the local zenith angle of the observations, indicative of more horizontal heterogeneity in the temperature and water vapor structure. This is not surprising considering that the geography of the region surrounding Poker Flat, Alaska, is quite variable, consisting of mountains and valleys.

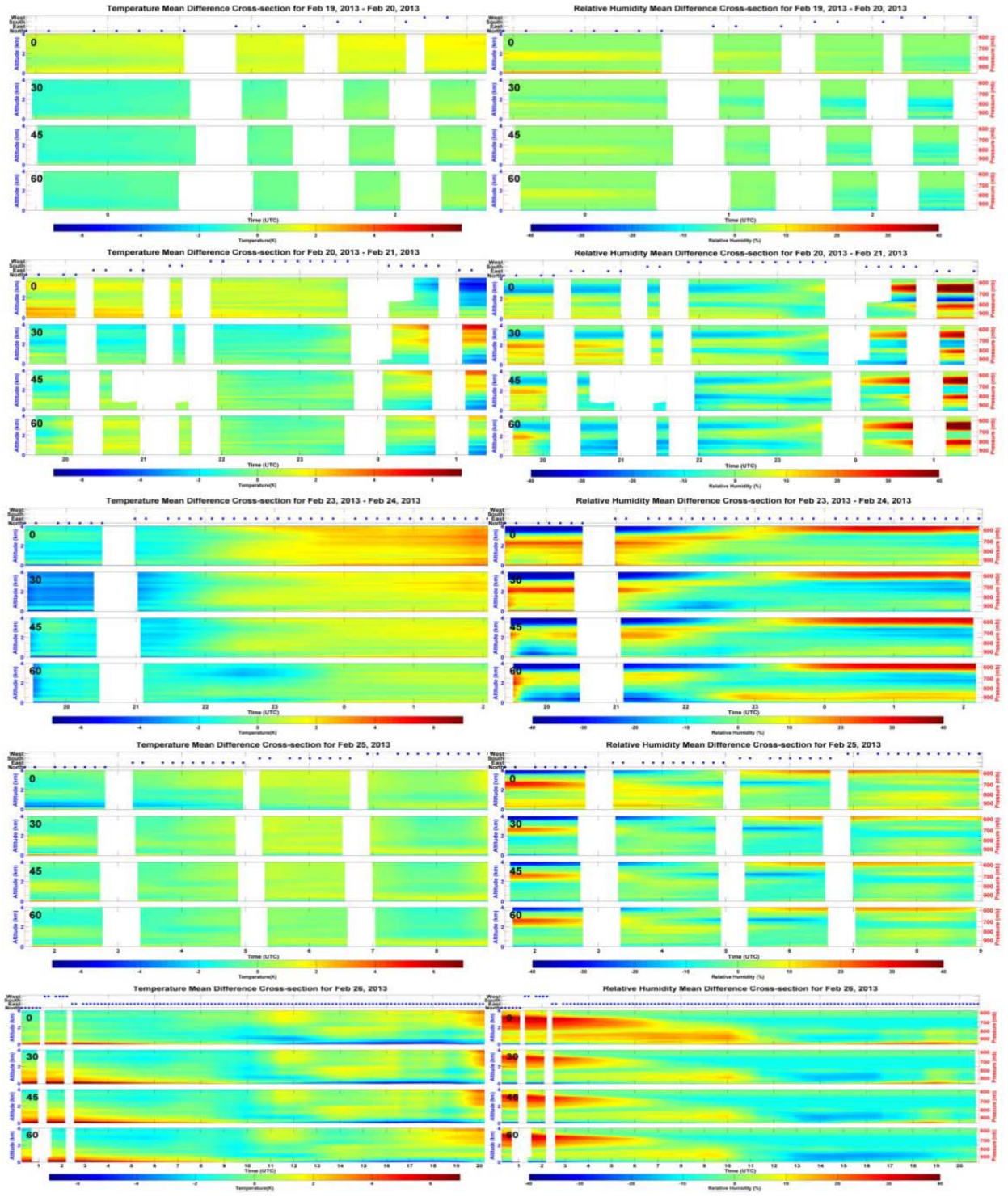

Figure 10. Time cross sections of the final ALOSE-2 ASSIST temperature and humidity profile deviations from the daily profile mean for the four different local zenith angles of measurement (0, 30, 45, and 60 degrees) with the indication of which of the four different azimuth angles (west, south, east, north) of the observation being viewed shown at the top of each figure.

4.3 ALOSE-3

Figure 11 shows the temperature and humidity cross sections for 24–25 April and 27–28 April 2013. It can be seen by comparing the GFS model panels with the final ASSIST panels that the model did capture the major features of the atmospheric structure in this case. However, there are some details, particularly in relative humidity such as the dry air in the PBL between 25–35 hrs. on the 27–28 April panel, which is actually the period 0100–1100 UTC of 28 April. It can be seen that the moisture increased significantly during the 5-day period of the measurements.

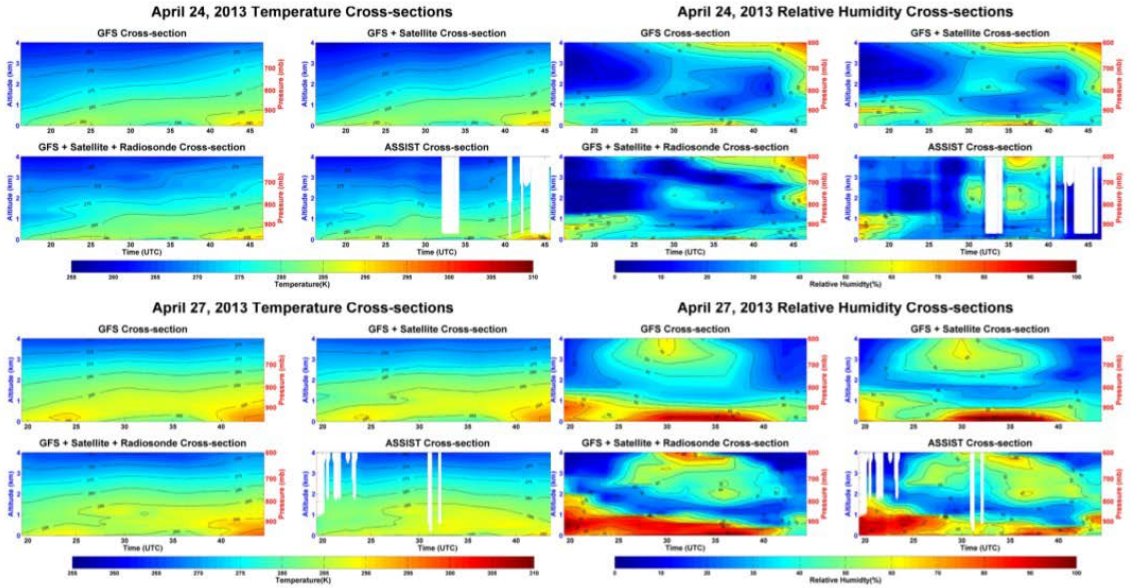

Figure 11. Temperature and humidity time section inputs (i.e., GFS model, satellite, and radiosonde) for obtaining the final ASSIST best estimate of the atmospheric state of the lower troposphere (0–4 km) for ALOSE-2; 24–25 April and 27–28 April 2013.

Figures 12 and 13 shows time cross sections of the final ALOSE-3 ASSIST temperature and humidity profile deviations from the daily profile mean for the four different local zenith angles of measurement (0, 30, 45, and 60 degrees) with the indication of which of the four different azimuth angles (west, south, east, north) of the observation being viewed shown at the top of each figure. Similar to ALOSE-1, for the April SGP data of ALOSE-3, we do not see a significant dependence on the local zenith or azimuth angle of the observations, indicative that the atmosphere was horizontally homogenous within the 4 km range of the ASSIST measurements (i.e., there is little line-of-site dependence on the atmospheric state).

Figure 14 shows a comparison of final ASSIST temperature profile retrievals and radiosonde profile measurements at the SGP ARM site during April for six different radiosonde release times during the 24–25 April 2013 time period. As can be seen the agreement is good except for the 1130 UTC sounding on 24 April. In this case, the radiosonde seems to be inconsistent with the other radiosonde measurements as well as the ASSIST final sounding both in the upper troposphere as well as in the lower troposphere. In any case, this example shows the ability of the final ASSIST product, which incorporates the radiosonde data, to deviate significantly from that data input when it is inconsistent with the other data being used to produce the final profiles.

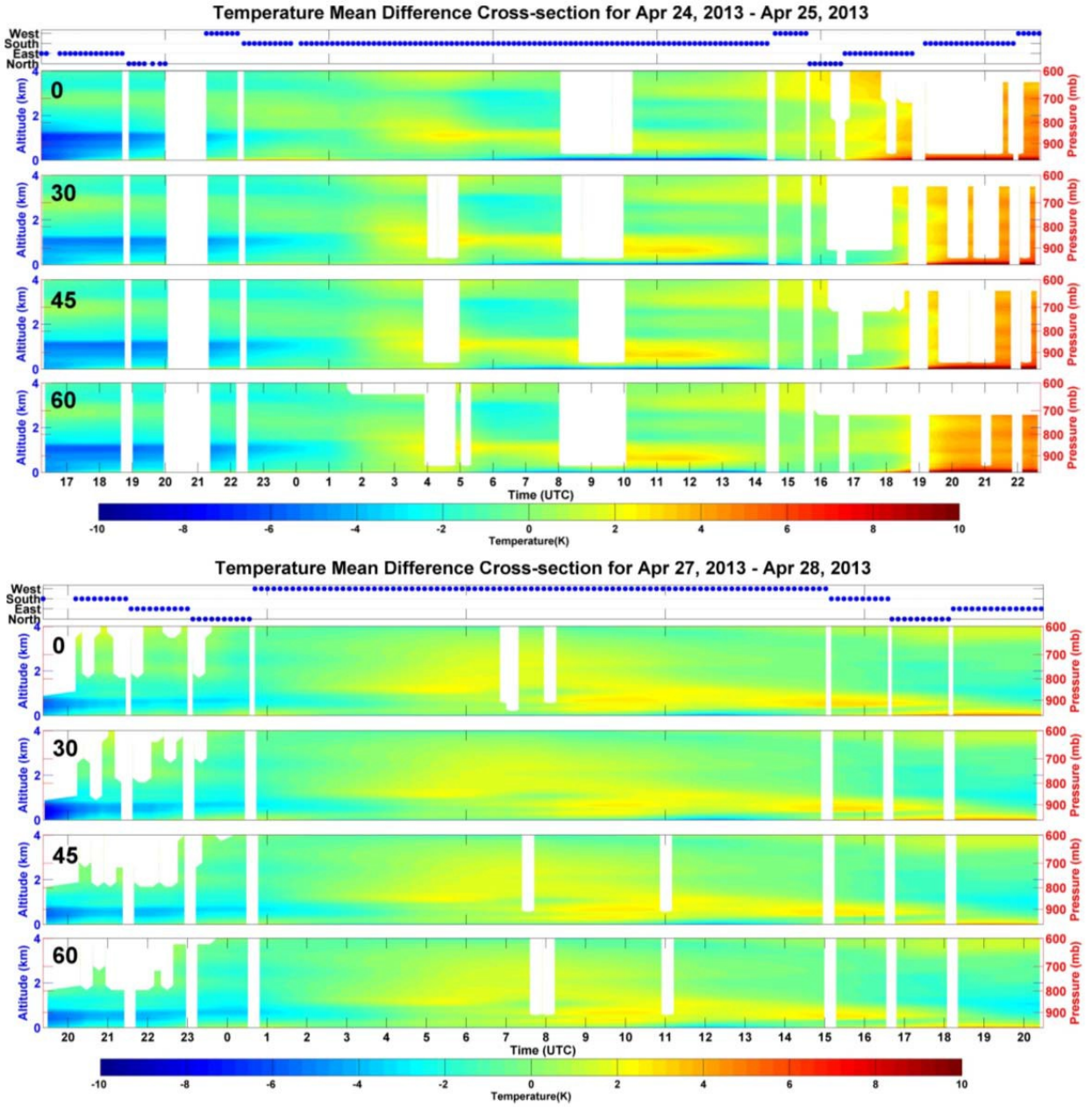

Figure 12. Time cross sections of the final ALOSE-3 ASSIST temperature profile deviations from the daily profile mean for the four different local zenith angles of measurement (0, 30, 45, and 60 degrees) with the indication of which of the four different azimuth angles (west, south, east, north) of the observation being viewed shown at the top of each figure.

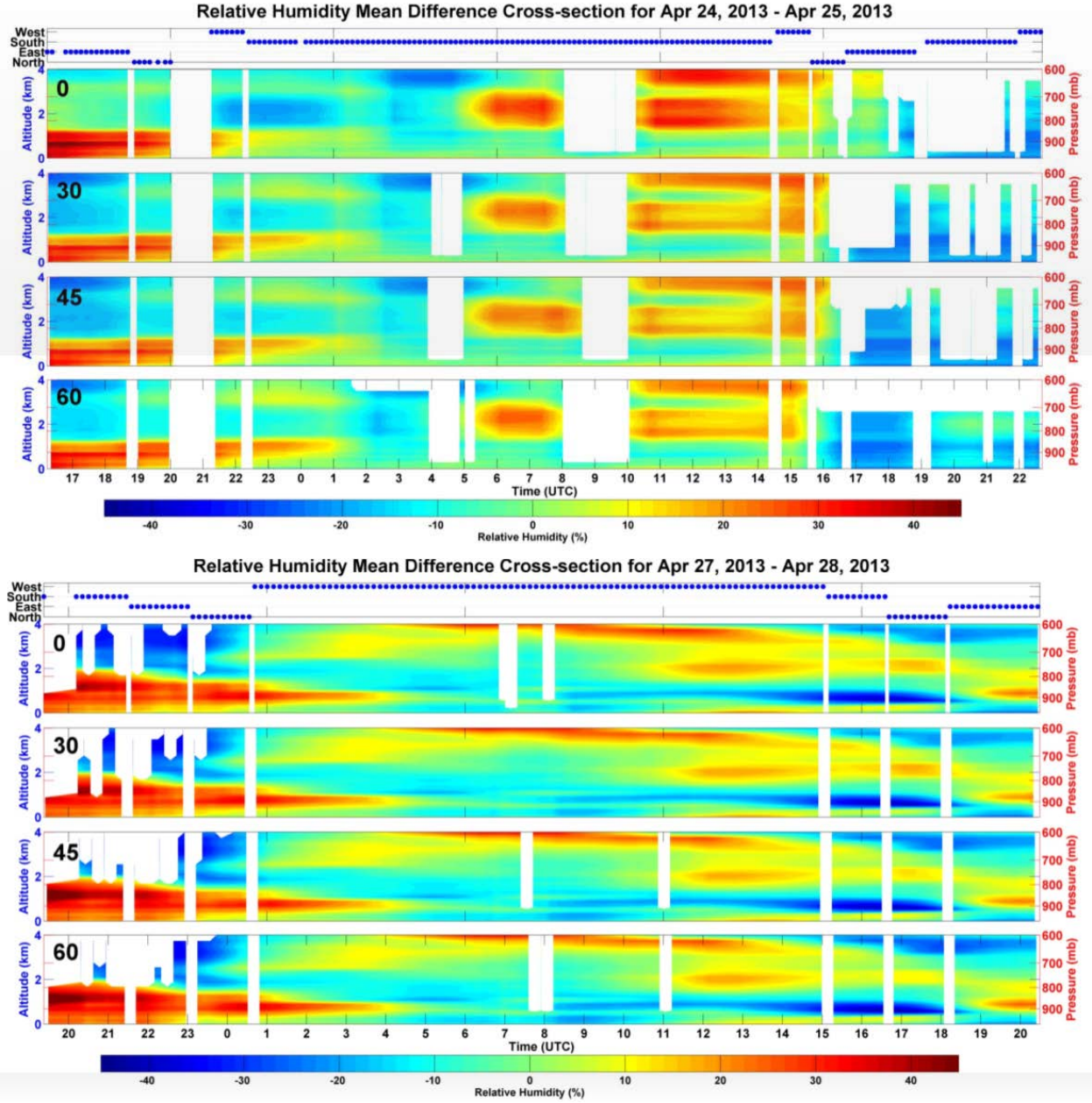

Figure 13. Time cross sections of the final ALOSE-3 ASSIST relative humidity profile deviations from the daily profile mean for the four different local zenith angles of measurement (0, 30, 45, and 60 degrees) with the indication of which of the four different azimuth angles (west, south, east, north) of the observation being viewed shown at the top of each figure.

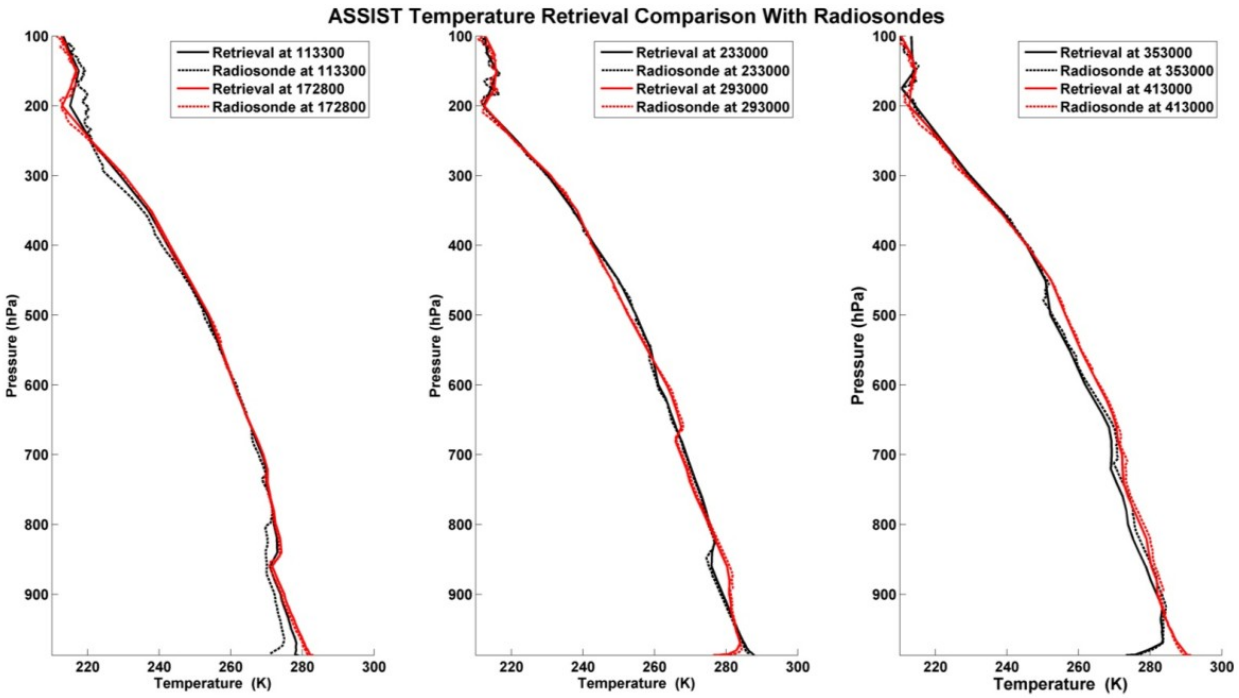

Figure 14. Comparison of final ASSIST temperature profile retrievals and radiosonde profile measurements at the SGP ARM site for six different radiosonde release times during the 24–25 April 2013 time period.

4.4 ALOSE-4

Figure 15 shows temperature and humidity cross sections for 10–14 July 2013. Although there is little variation in atmospheric temperature during this period, it can be seen by comparing the GFS model panels with the final ASSIST panels that the model temperature lapse rate in the low troposphere is too small (i.e., temperature decreases too slowly with altitude) as compared to that shown by the final ASSIST panels. Also, the model humidity fails to show important vertical structure variations shown by the final ASSIST product. This is particularly noticeable for the 12–13 July panel (i.e., panel 6 of Figure 15) where the final ASSIST product shows four distinct layers of high moisture but the model only shows two layers of relatively high moisture concentration.

Figure 16 shows time cross sections of the final ALOSE-4 ASSIST temperature and humidity profile deviations from the daily profile mean for the four different local zenith angles of measurement (0, 30, 45, and 60 degrees) with the indication of which of the four different azimuth angles (west, south, east, north) of the observation shown at the top of each figure. We can see that the July SGP temperature data of ALOSE-4 does not show much dependence on the local zenith or azimuth angle of the observations within the 4 km range of the ASSIST measurements (i.e., there is little line-of-site dependence on the atmospheric temperature). However, with the exception of 12–13 July, this is not the case for atmospheric humidity where there are significant variations with local zenith angle for certain time periods of the day for each of three of the four observation days. A high horizontal variability on atmospheric humidity is expected for the SGP during July because there is generally intense convection during most days of that month.

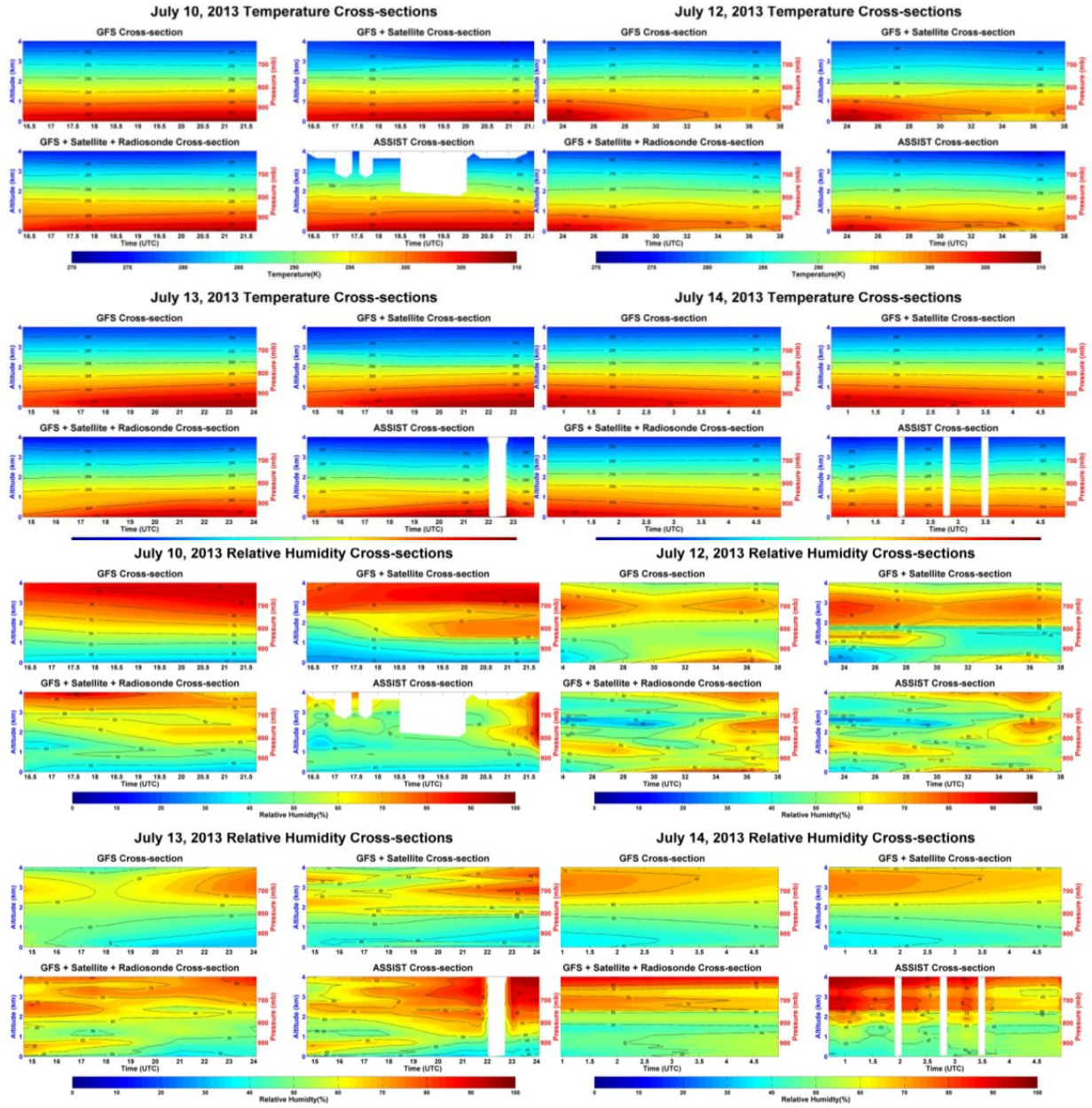

Figure 15. Temperature and humidity time section inputs (i.e., GFS model, satellite, and radiosonde) for obtaining the final ASSIST best estimate of the atmospheric state of the lower troposphere (0–4 km) for ALOSE-4; 10, 12, 13, and 14 July 2013.

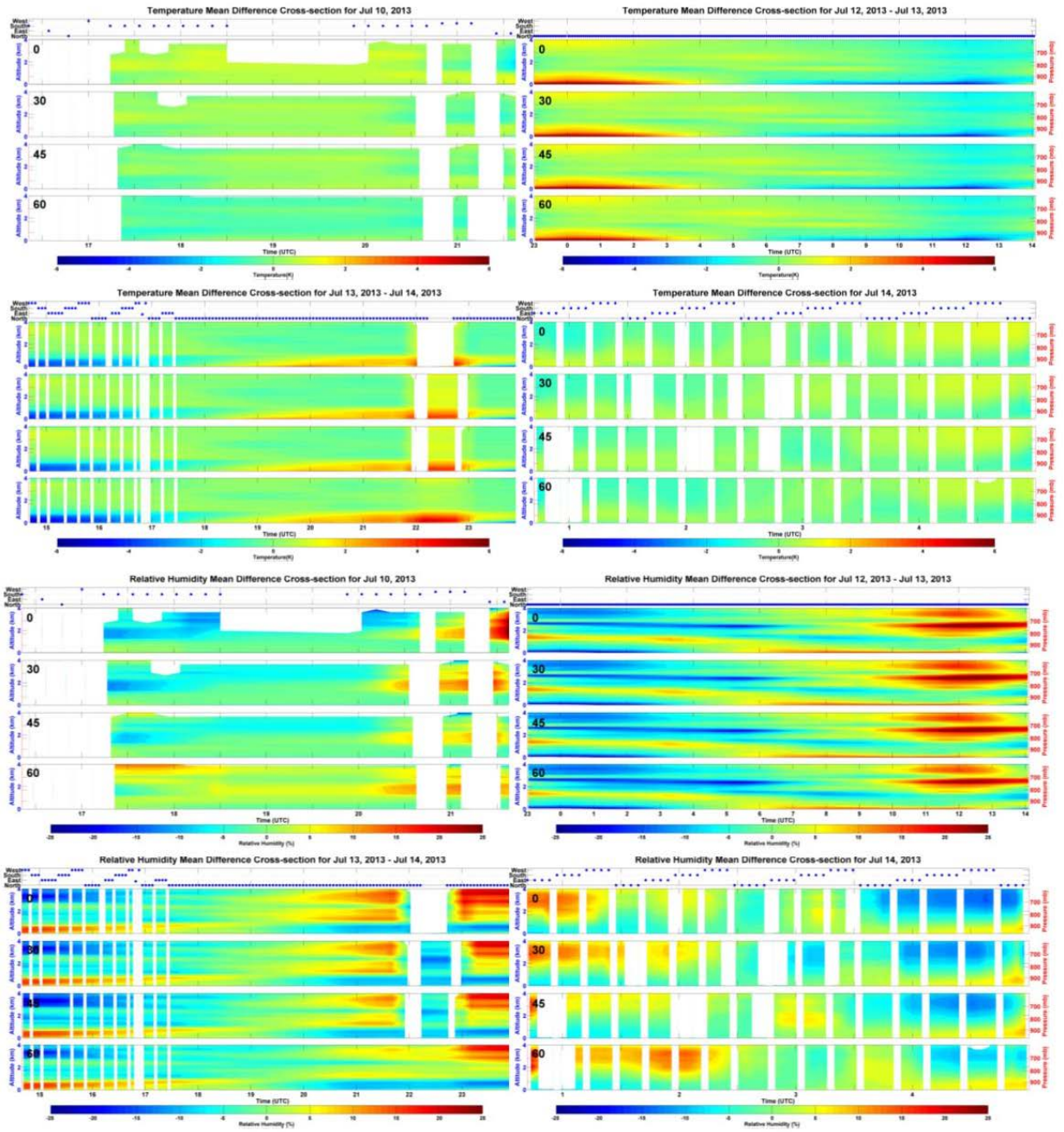

Figure 16. Time cross sections of the final ALOSE-4 ASSIST relative humidity profile deviations from the daily profile mean for the four different local zenith angles of measurement (0, 30, 45, and 60 degrees) with the indication of which of the four different azimuth angles (west, south, east, north) of the observation being viewed shown at the top of each figure.

Figure 17 shows comparisons of the final ASSIST retrievals with radiosondes released at six different times on 13 July 2013. It can be seen that the final ASSIST retrievals faithfully reproduce the radiosonde-observed vertical structure with the exception of the very near surface on 13 July at 113100 UTC. However, it is expected that the ASSIST temperature measurements for the lowest 1 km are more accurate than the radiosonde measurements in this near-surface layer due to the rapid rise of the balloon once it is released from the ground.

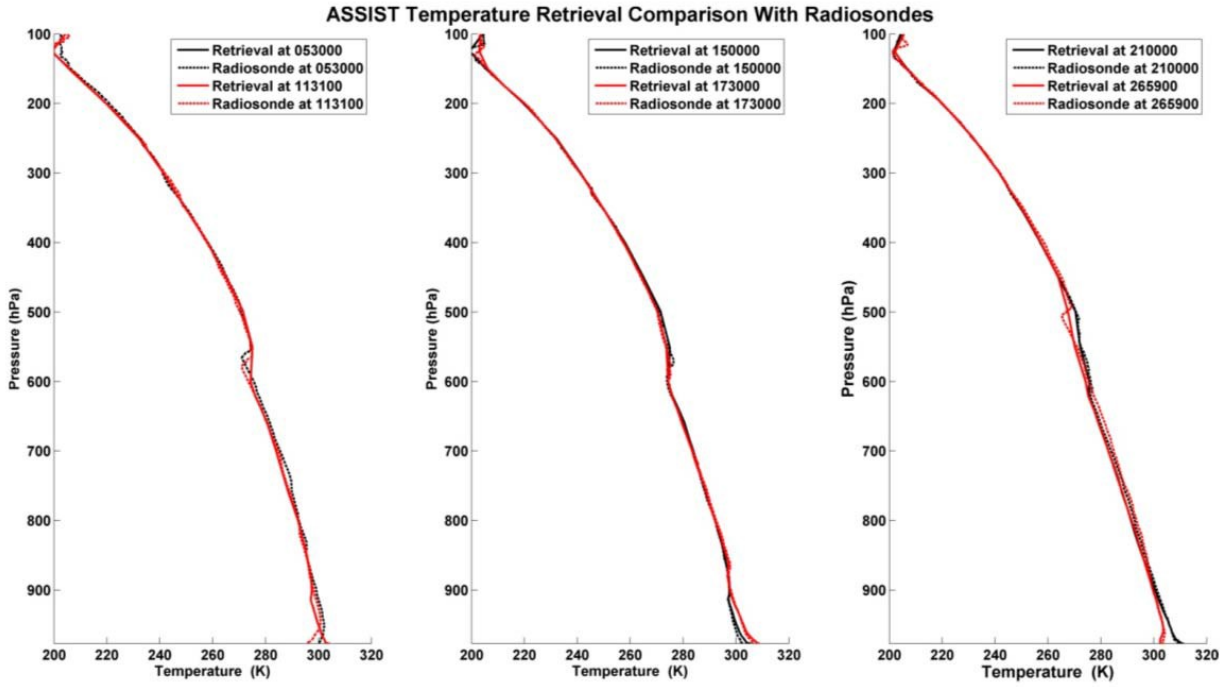

Figure 17. Comparison of final ASSIST temperature profile retrievals and radiosonde profile measurements at the SGP ARM site for six different radiosonde release times during 13 July 2013.

4.5 ALOSE-5

Figure 18 shows the temperature and humidity cross sections for 27 September to 3 October 2013 obtained during ALOSE-5. Once again, there is little variation in atmospheric temperature during this period and the GFS model panels compare favorably with the final ASSIST panels. However, the model humidity deviates significantly from the final ASSIST product. This is particularly noticeable for the 1 October panel where the final ASSIST product shows a lot of moisture structure not shown by the model but validated by the radiosonde profile data (see the last four panels of Figure 18).

Figure 19 shows time cross sections of the final ALOSE-5 ASSIST temperature and humidity profile deviations from the daily profile mean for the four different local zenith angles of measurement (0, 30, 45, and 60 degrees) with the indication of which of the four different azimuth angles (west, south, east, north) of the observation shown at the top of each figure. We can see that the TWP temperature data of ALOSE-5 does not show much dependence on the local zenith or azimuth angle of the observations within the 4 km range of the ASSIST measurements (i.e., there is little line-of-site dependence on the atmospheric temperature). However, the 30 September–1 October case shows significant dependence on local zenith angle for atmospheric humidity, particularly in the 13–21 UTC time period.

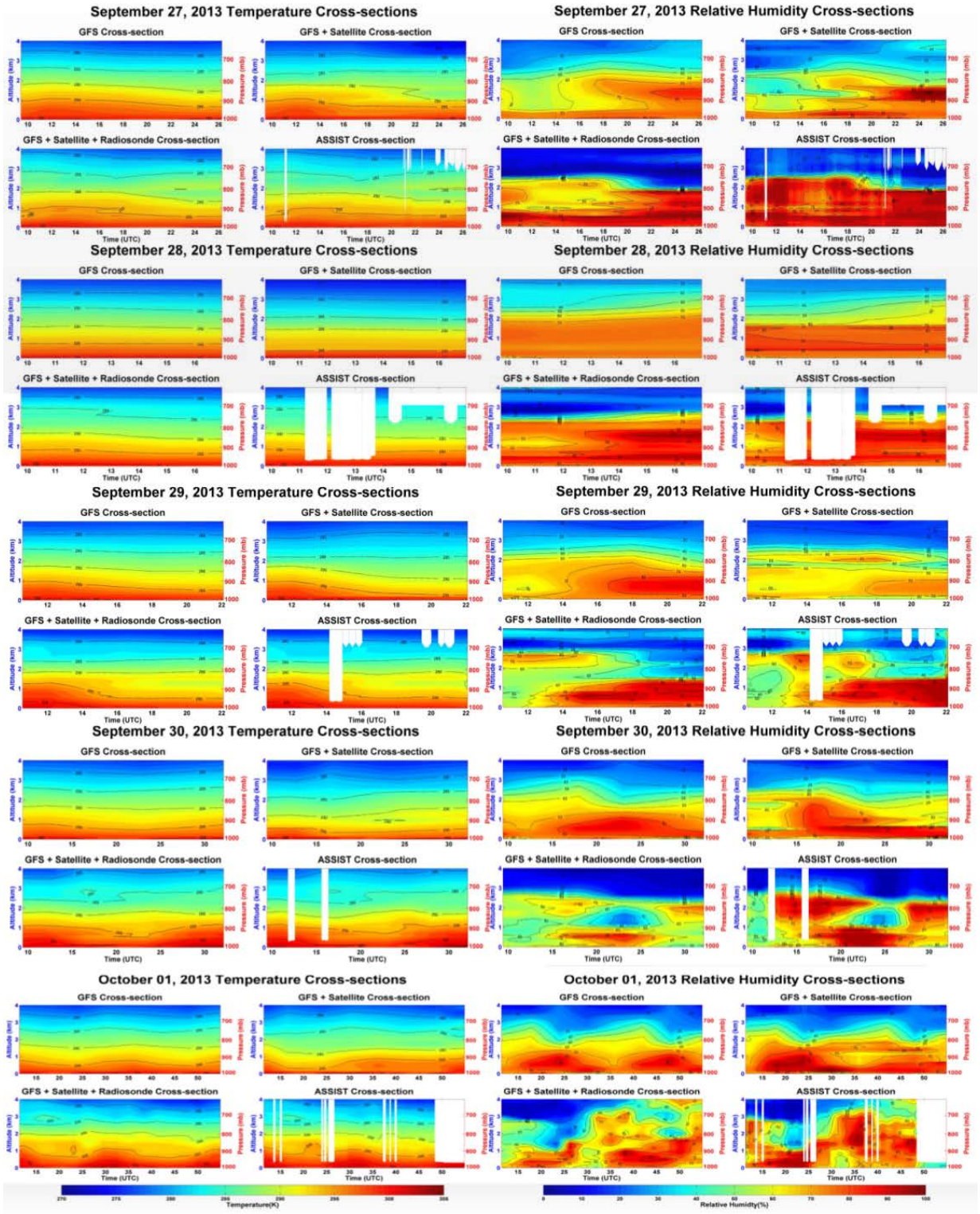

Figure 18. Temperature and humidity time section inputs (i.e., GFS model, satellite, and radiosonde) for obtaining the final ASSIST best estimate of the atmospheric state of the lower troposphere (0–4 km) for ALOSE-5; 27, 28, 29, and 30 September and 1 October 2013.

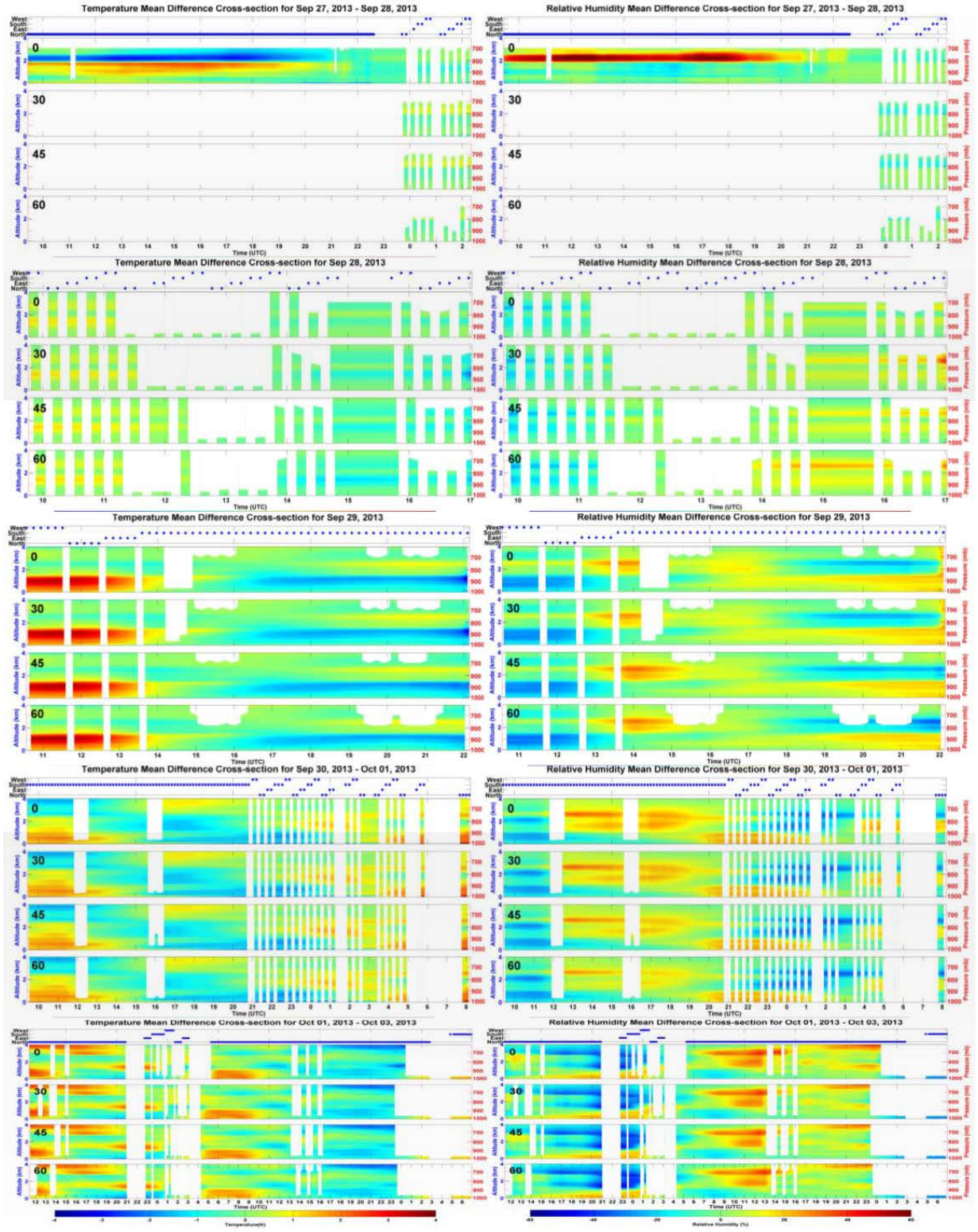

Figure 19. Time sections of the final ALOSE-5 ASSIST temperature and humidity profiles deviation from daily mean for four different zenith angles (0, 30, 45, and 60 degrees).

Figure 20 shows the comparison of final ASSIST temperature profile retrievals and radiosonde profile measurements at the TWP Darwin, Australia, ARM site for three different radiosonde release times during 27 September 2013. The agreement between the final ASSIST product and the radiosonde observations is excellent for this day providing assurance that the TWP ALOSE-5 data set possesses high accuracy.

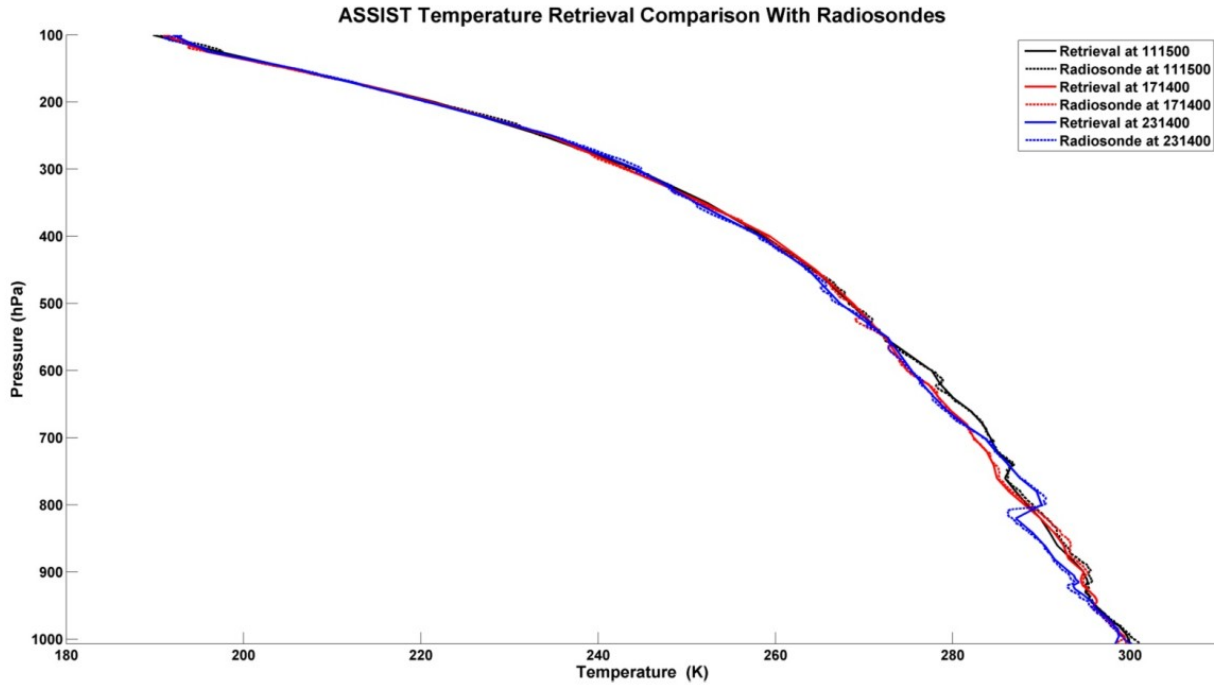

Figure 20. Comparison of final ASSIST temperature profile retrievals and radiosonde profile measurements at the TWP Darwin, Australia, ARM site for three different radiosonde release times during 27 September 2013.

5.0 Public Outreach

Public outreach was conducted at the University of Alaska-Fairbanks with a lecture to students entitled "IR FTS Remote Sensing of Atmospheric Profiles." Also, a presentation to personnel of the NOAA Alaskan Region Weather Service Forecast Office entitled "JPSS PG Alaska - AIRS, IASI, and CrIS Retrievals."

6.0 ALOSE Publications

6.1 Journal Articles/Manuscripts

Smith WL Sr., S Green, M Howard, and M Yesalusky, "Atmospheric Line of Site Experiment (ALOSE)-An experiment to obtain detailed atmospheric thermodynamic structure for numerical weather prediction model validation." In preparation for publication in the *Journal of Applied Meteorology and Climatology*, 2015.

Smith WL, A Larar, M Goldberg, X Liu, H Revercomb, E Weisz, M Yesalusky and D Zhou. 2014. "The May 2013 SNPP Cal/Val Campaign: validation of satellite soundings." In *Proceedings of SPIE, Multispectral, Hyperspectral, and Ultraspectral Remote Sensing Technology, Techniques and Applications V*, Vol. 9263, pp. 92630W–92630W-10. October 14–16, 2014, Beijing, China. DOI 10.1117/12.2069500. The International Society for Optical Engineering, Bellingham, Washington.

6.2 Meeting Abstracts/Presentations/Posters

Smith WL Sr. 2013. "Global Atmospheric Profiling Techniques for the Improvement & Increased Utility of Atmospheric Compensation Methods." Department of Energy University & Industry Technical Interchange Review Meeting, Lansing Center, Lansing Michigan, June 4–6, 2013.

Smith WL Sr., M Yesalusky, and E Weisz. 2013. "Ultraspectral Satellite Soundings – Validation Using Ground-based Spectrometer Measurements" 2013 EUMETSAT Meteorological Satellite Conference 19th American Meteorological Society (AMS) Satellite Meteorology, Oceanography and Climatology Conference, September 16–20, 2013, Hofburg, Vienna, Austria.

Smith WL Sr., A Larar, M Goldberg, X Liu, H Revercomb, E Weisz, M Yesalusky and D. Zhou, "The May 2013 SNPP Cal/Val Campaign – Validation of Satellite Soundings." SPIE Asia Pacific Remote Sensing Symposium, October 13–16, 2014, Beijing International Convention Center, Beijing, China.

7.0 References

Pierce RB, JA Al-Saadi, T Schaack, A Lenzen, T Zapotocny, D Johnson, C Kittaka, M Buker, MH Hitchman, G Tripoli, TD Fairlie, JR Olson, M Natarajan, J Crawford, J Fishman, M Avery, EV Browell, J Creilson, Y Kondo and ST Sandholm. 2003. "Regional Air Quality Modeling System (RAQMS) predictions of the tropospheric ozone budget over east Asia." *Journal of Geophysical Research: Atmospheres* 108(D21).

Rochette L, WL Smith, M Howard and T Bratcher. 2009. "ASSIST, Atmospheric Sounder Spectrometer for Infrared Spectral Technology: Latest development and improvement in the atmospheric sounding technology (Invited Paper)." In *Proceedings of SPIE, Imaging Spectrometry XIV, Vol. 7457*, pp. 7457-01. August 3-4, 2009, San Diego, California. DOI 10.1117/12.829344. The International Society for Optical Engineering, Bellingham, Washington.

Rodgers CD. 1976. "Retrieval of atmospheric temperature and composition from remote measurements of thermal radiation." *Reviews of Geophysics* 14(4):609-624.

Smith WL, WF Feltz, RO Knuteson, HE Revercomb, HM Woolf and HB Howell. 1999. "The Retrieval of Planetary Boundary Layer Structure Using Ground-Based Infrared Spectral Radiance Measurements." *Journal of Atmospheric and Oceanic Technology* 16(3):323-333.

www.arm.gov

U.S. DEPARTMENT OF
ENERGY

Office of Science